

A Research and Educational Robotic Testbed for Real-Time Control of Emerging Mobility Systems

From Theory to Scaled Experiments

BEHDAD CHALAKI, LOGAN E. BEAVER, A.M. ISHTIAQUE MAHBUB, HEESEUNG BANG,
and ANDREAS A. MALIKOPOULOS 

Emerging mobility systems, for example, connected and automated vehicles (CAVs), shared mobility, and electric vehicles, mark a paradigm shift in which myriad opportunities exist for users to better monitor transportation network conditions and make optimal operating decisions to improve safety and reduce pollution, energy consumption, and travel delays [1]. As we move to increasingly complex emerging mobility systems, new control approaches are needed to optimize the impact on the system behavior [2] of the interplay among vehicles in different traffic scenarios [3]. Several studies have shown the benefits of CAVs to reduce energy consumption and alleviate traffic congestion in specific transportation scenarios [4], [5], [6]. There have been two major approaches to utilizing CAVs, namely, platooning and traffic smoothing. A platoon is defined as a group of closely coupled vehicles traveling to reduce their aerodynamic drag, especially at high cruising speeds. The concept of platoon formation is a popular system-level approach to address traffic congestion, which gained momentum in the 1980s and 1990s [7], [8], [9]. There has been a rich body of research exploring various methods of forming and/or utilizing platoons to improve transportation efficiency [10], [11], [12], [13], [14], [15], [16], [17], [18], [19], [20], [21], [22].

Traffic smoothing is another approach that has been explored to mitigate the speed variation of individual vehicles throughout the transportation network, which may be introduced by unnecessary braking and the topology of the road network. One of the very early efforts in this direction was proposed by Athans [23] for the safe and efficient coordination of merging maneuvers, with the intention of avoiding congestion. Assuming a given merging sequence, Levine and Athans formulated the merging problem as a linear optimal regulator [24] to control a single string of vehicles, with the aim of minimizing the speed errors that will affect the desired headway between each consecutive pair of vehicles. Since then, several studies have been reported in the literature that investigate traffic smoothing

to eliminate stop-and-go driving in traffic scenarios such as single intersections [25], [26], [27], [28], [29], [30], [31], [32], [33], [34], [35], [36], [37], [38], [39], [40], [41], [42], [43], [44], [45], [46], [47], [48], [49], [50], [51], [52], [53], [54], [55], [56], multiple adjacent intersections [53], [57], [58], [59], [60], [61], [62], [63], [64], [65], [66], merging roadways [67], [68], [69], [70], [71], [72], [73], [74], [75], roundabouts [5], [76], [77], [78], [79], [80], [81], [82], speed reduction zones and lane drops [83], [84], [85], [86], [87], [88], [89], [90], [91], and transportation corridors [92], [93], [94], [95], [96], [97], [98]. Two recent survey articles [99], [100] provide a comprehensive review of the state-of-the-art methods and challenges in this area.

Commercial simulation platforms are currently available for testing and validating control algorithms for CAVs in a safe and cost-efficient setting. Simulation can help us gather key information about how the system performs in an idealized environment. However, evaluating the performance of CAVs in a simulation environment imposes limitations since modeling the exact vehicle dynamics and driving behavior is not feasible. Capturing the complexities arising from data loss and transmission latency associated with connectivity and communication networks can be also challenging. As Grim et al. [101] stated, “*the problem with simulations is that they are doomed to succeed.*” Although there have been several studies reporting on the impact of the coordination of CAVs in traffic scenarios, for example, intersections, merging at roadways, and roundabouts, the effectiveness of these approaches has been mostly shown in simulation. Therefore, validating control approaches for CAVs in a physical testbed is of great importance.

Scaled testbeds for CAVs have attracted considerable attention over the past few years. Such testbeds can be used to conduct quick and repeatable experiments in an effort to go one step beyond simulation. Gulliver [102] and Moped [103] have been the outcome of early efforts on developing scaled testbeds for robotic vehicles. Gulliver’s focus is mainly on communication among vehicles, while Moped is focused on the low-level control of a single scaled vehicle. The Massachusetts Institute of Technology’s (MIT’s) Duckietown [104] employs differential drive robots, and Go-chart [105] uses four-wheel skid-steer vehicles. Both testbeds

focus primarily on local perception and autonomy. Cambridge Minicars [106] constitute another testbed for emulating cooperative driving in highway traffic conditions. A general-purpose robotic testbed, called Robotarium, has been developed [107], which features differential drive robots. The Cyber-Physical Mobility Lab [108] has implemented another scaled testbed on decision-making policies and trajectory planning. For a relatively recent review of such robotics testbeds, see [109].

In 2017, we established the Information and Decision Science Lab Scaled Smart City (IDS³C) to develop and validate control algorithms for emerging mobility systems. IDS³C occupies a 20 × 20-ft area. It includes 50 robotic cars and 10 aerial vehicles and can replicate real-world traffic scenarios in a small and controlled environment. This testbed can help us prove concepts beyond the simulation level and understand the implications of errors/delays in vehicle-to-vehicle and vehicle-to-infrastructure communication as well as their impact on energy usage. IDS³C can help us implement control algorithms for coordinating CAVs in different traffic scenarios, such as intersections, merging roadways, speed reduction zones, roundabouts, and transportation corridors. IDS³C also includes driver emulation stations interfaced directly with the cars, which allow for exploring human driving behavior. The robotic cars share many features with full-scale cars, such as a built-in suspension and an Ackermann steering mechanism.

There are several features that distinguish IDS³C from other testbeds. First, unlike MIT's Duckietown [104] and Go-chart [105], the CAVs in IDS³C resemble full-scale vehicles by using four wheels, a built-in suspension, and an Ackermann steering mechanism. Second, in contrast to the scaled testbeds reported in [104], [106], [107], and [108], IDS³C is equipped with driver emulation stations that interface directly with the robotic cars. These stations enable the exploration and study of human driving behavior and their interactions with CAVs. Being able to study how CAVs can safely interact and coexist with human-driven vehicles is of great importance since different penetration rates of CAVs can significantly alter transportation efficiency and safety. Third, rather than focusing on specific scenarios in a transportation network [102], [106] or a single individual vehicle [103], IDS³C can accommodate almost every possible traffic scenario, including crossing three- and four-way intersections, merging at roadways and roundabouts, cruising in congested traffic, passing through speed reduction zones, and lane-merging and passing maneuvers. These features make IDS³C a unique scaled robotic testbed to study problems in emerging mobility systems, such as the coordination of CAVs, shared mobility, eco-routing, and first/last-mile delivery. Finally, only a few testbeds [104], [108] are equipped with a "digital twin." The digital twin of IDS³C, called IDS Scaled Smart Digital City (3D City), is a Unity-based virtual simulation environment that can operate alongside the physical IDS³C and interface with

the existing control framework. IDS 3D City provides the framework to develop and implement control algorithms for emerging mobility systems in simulation before moving to the physical IDS³C for validation. More details about IDS 3D City can be found in [110].

In what follows (see "Summary"), we start our exposition by providing a brief description of the hardware and software architecture of IDS³C. Then, we present an overview of a real-time coordination framework for CAVs that has been implemented and validated in IDS³C and field testing [98], [111]. Next, we present a tutorial of this framework in an application to a multilane roundabout in IDS³C, using nine CAVs. Finally, we provide a demonstration study in IDS³C by using a fleet of 15 CAVs and show how we can improve traffic throughput along a transportation

Summary

Emerging mobility systems, for example, connected and automated vehicles (CAVs), shared mobility, and electric vehicles, provide the most intriguing opportunity for enabling users to better monitor transportation network conditions and make better decisions for improving safety and transportation efficiency. However, before connectivity and automation are deployed en masse, a thorough evaluation of CAVs is required, ranging from numerical simulation to real-world public roads. The assessment of the performance of CAVs in scaled testbeds has recently gained momentum due to the flexibility they offer to conduct quick repeatable experiments that could go one step beyond simulation. This article introduces the Information and Decision Science Lab Scaled Smart City (IDS³C), a 1:25 research and educational scaled robotic testbed that is capable of replicating different real-world urban traffic scenarios. IDS³C was designed to investigate the effect of emerging mobility systems on safety and transportation efficiency. On the educational front, IDS³C can be used for 1) training and educating graduate students by exposing them to a balanced mix of theory and practice, 2) integrating research outcomes into existing courses, 3) involving undergraduate students in research, 4) creating interactive educational demos, and 5) reaching out to high-school students. IDS³C has become a research and educational catalyst for motivating interest in undergraduate and high-school students in science, technology, engineering, and mathematics. In our exposition, we also present a real-time control framework that can be used to coordinate CAVs in traffic scenarios such as crossing signal-free intersections, merging at roadways and roundabouts, cruising in congested traffic, passing through speed reduction zones, and lane-merging and passing maneuvers. Finally, we provide a tutorial for applying our framework in coordinating robotic CAVs in a multilane roundabout scenario and a transportation corridor in IDS³C.

Several studies have shown the benefits of CAVs to reduce energy consumption and alleviate traffic congestion in specific transportation scenarios.

corridor, which consists of a roundabout, an intersection, and a merging roadway.

INFORMATION AND DECISION SCIENCE LAB SCALED SMART CITY

IDS³C (see Figure 1) is a 1:25 scaled robotic testbed spanning more than 400 ft², and it is capable of replicating real-world traffic scenarios in a small and controlled environment by using 50 ground and 10 aerial vehicles. IDS³C provides an opportunity to prove concepts beyond simulation and understand the implications of errors and delays in vehicle-to-vehicle and vehicle-to-infrastructure communication as well as their impact on energy usage. IDS³C can also be used to understand the implications of emerging mobility systems (consisting of CAVs, shared mobility, and electric vehicles) on safety and transportation efficiency. Another facet of research that can be explored using IDS³C is complex missions that include the cooperation of aerial and ground vehicles for logistic problems, such as last-mile delivery. IDS³C includes driver emulation stations [112] interfaced directly with the robotic cars for the exploration of human driving behavior.



FIGURE 1 A view of the Information and Decision Science Lab Scaled Smart City, with connected and automated vehicles coordinating at an intersection.

IDS³C is equipped with a Vicon motion capture system and uses eight cameras to track the position of each vehicle, with submillimeter accuracy. The testbed contains a dozen traffic scenarios, including merging roadways, multilane roundabouts, adjacent intersections, multilane intersections, lane drops, and speed reduction zones. A central mainframe computer (processor: Intel Core i7-6950X CPU at 3 GHz × 20; memory: 128 GB) stores a map of IDS³C as a database of line and arc segments that make up the road network. The coordination of the CAVs within IDS³C is achieved using a multilevel control framework spanning the mainframe computer and the individual CAVs in an experiment. Each CAV is given its own thread on the central mainframe computer. The latter communicates the vehicle's position through Vicon and generates its trajectory. Lane and reference trajectory tracking are accomplished onboard each CAV in a purely distributed manner.

We developed IDS³C with the capacity to experimentally validate a wide variety of urban mobility scenarios. This includes eco-routing, mixed traffic [5], [113], last-mile delivery [114], and air-ground coordination [115]. In several recent efforts, we have used IDS³C to implement and validate control algorithms for coordinating CAVs in traffic scenarios such as merging roadways [71], roundabouts [79], intersections [42], adjacent intersections [60], [61], [62], and corridors [116]. We have also used IDS³C to transfer policies from neural networks [81], [82] and handle the stochasticity that arises in physical systems [117]. IDS³C is in a position to provide a means for user interaction through a mobile application, which enables submitting origin-destination travel requests for dynamic routing in shared mobility and last-mile delivery scenarios.

More recently, we introduced a Unity-based virtual simulation environment for emerging mobility systems, called IDS 3D City, intended to operate alongside its physical peer, IDS³C, and interface with the existing control framework. For a brief summary of IDS 3D City, see "Information and Decision Science Lab Scaled Smart Digital City." For further technical details, see [110]. We have used IDS³C to develop a control framework for the real-time coordination of CAVs in different traffic scenarios, such as crossing signal-free intersections, merging at roadways and roundabouts, cruising in congested traffic, passing through speed reduction zones, and lane-merging and passing maneuvers. Next, we outline the main features of this framework.

CONTROL FRAMEWORK FOR COORDINATION OF CONNECTED AND AUTOMATED VEHICLES

IDS³C has been extensively used for the development and implementation of control algorithms aimed at coordinating CAVs in different traffic scenarios. By coordinating CAVs in traffic scenarios, the vehicles do not have to come to a full stop, thereby conserving momentum and fuel while also improving travel time. In this context, safety

is explicitly guaranteed by imposing constraints on each vehicle, including rear-end safety, a maximum speed limit, and lateral collision avoidance.

Several research efforts have considered a two-level optimization framework for coordinating CAVs, consisting of a travel time minimization (upper level) and an energy minimization problem (lower level). For each CAV with a given origin–destination, the solution of the upper-level problem yields the travel time for the CAV to exit a “control zone,” inside of which CAVs can communicate with one another. The solution of the low-level problem yields, for each CAV, the control input (acceleration/deceleration) to achieve the solution of the upper-level problem while minimizing energy consumption, subject to the state, control, and safety constraints. The details of the low-level problem can be found in [34], [47], and [118]. Solving a constrained optimal control problem leads to a system of nonlinear equations that are often infeasible to solve in real time. For more details on the constrained optimal control and the associated technical

challenges, see “The Challenge With Constrained Optimal Control.” To avoid the challenges associated with constrained optimal control, we have proposed an alternative control framework consisting of a single-level optimization aimed at both minimizing energy consumption and improving traffic throughput [47]. Next, we highlight the features of this framework.

Problem Formulation

Although the control framework outlined here can be applied to any traffic scenario, we use an intersection as a reference to provide the fundamental ideas. This is because an intersection has unique features that make it technically more challenging compared to other traffic scenarios. However, our analysis can be applied to other traffic scenarios. We consider CAVs at a 100% penetration rate that are crossing a signal-free intersection (see Figure 2). The region at the center of the intersection, called the *merging zone*, is the area of potential lateral collision of the CAVs. The intersection has a *control zone*, inside of which the CAVs plan their

Information and Decision Science Lab Scaled Smart Digital City

The Information and Decision Science Lab (IDS) Scaled Smart Digital City (3D City) is a digital replica of the IDS Scaled Smart City (IDS³C) that uses AirSim and Unity. We have designed IDS 3D City to integrate the control framework used in IDS³C to simulate virtual vehicles. IDS 3D City enables users to rapidly iterate their control algorithms and

experiment parameters before deploying them to IDS³C. A schematic of how IDS 3D City interacts with IDS³C is available in Figure S1. The end result is a transition between physical and virtual environments, with minimal changes to input files as well as the capability to mix physical and virtual vehicles.

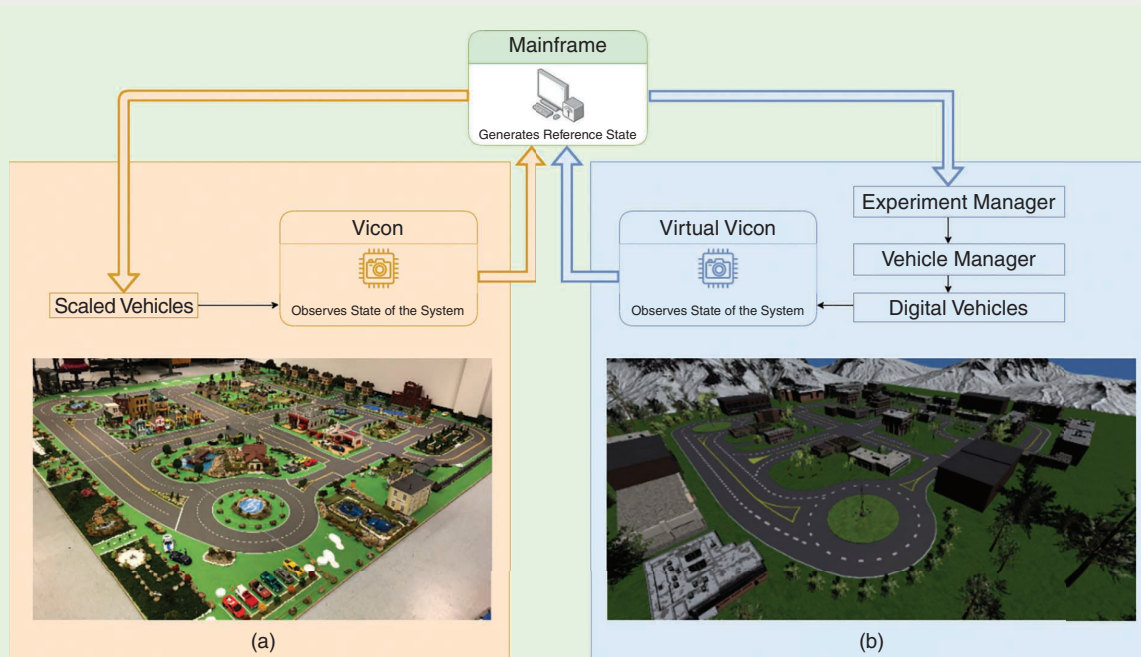


FIGURE S1 The (a) physical and (b) virtual city environments. The mainframe computer can switch between physical and virtual experiments.

The Challenge With Constrained Optimal Control

The standard methodology to solve a continuous-time constrained optimal control problem is to employ Hamiltonian analysis with interior point state and/or control constraints [S1]. Namely, we first start with the unconstrained arc and derive the solution of the optimal control problem without considering any of the state or control constraints. If the unconstrained solution violates any of the state and control constraints, then the unconstrained arc is pieced together with the arc corresponding to the violated constraint. The two arcs yield a set of algebraic equations that are solved simultaneously using the boundary conditions and optimality conditions between the arcs. If the resulting solution, which includes the determination of the optimal switching time from one arc to the next one, violates another constraint, then the last two arcs are pieced together with the arc corresponding to the new violated constraint, and we solve again the problem with the three arcs pieced together. The three arcs will yield a new set of algebraic equations that need to be solved, and this process is repeated until the solution does not violate any constraints. This iterative process can be computationally intensive for several reasons. First, the Euler–Lagrange equations are numerically unstable for nonconservative systems, leading to significant numerical challenges [S2]. Second, the number of active constraints is not known a priori, and it may require a significant

number of iterations to compute. Third, the boundary conditions and recursive equations may be implicit functions that do not have a closed-form analytical solution.

Excluding cases with terminal speed and safety constraints, in recent work [118], [S3], we have introduced a condition-based solution framework for the optimal coordination of connected and automated vehicles, which leads to a closed-form analytical solution without this iterative procedure. In this framework, we mathematically characterize the activation cases of different state and control constraint combinations and provide a set of a priori conditions under which different constraint combinations can become active. Although this approach alleviates the computational complexity of the constrained optimal control in the coordination problem to some extent, the aforementioned iterative procedure is still required for cases when safety and terminal speed constraints are included.

REFERENCES

- [S1] A. E. Bryson and Y. C. Ho, *Applied Optimal Control: Optimization, Estimation and Control*. Boca Raton, FL, USA: CRC Press, 1975.
 [S2] A. E. Bryson, "Optimal control—1950 to 1985," *IEEE Control Syst. Mag.*, vol. 16, no. 3, pp. 26–33, Jun. 1996, doi: 10.1109/37.506395.
 [S3] A. M. I. Mahbub and A. A. Malikopoulos, "Conditions for state and control constraint activation in coordination of connected and automated vehicles," in *Proc. 2020 Amer. Control Conf.*, pp. 436–441, doi: 10.23919/ACC45564.2020.9147842.

time trajectories (a time trajectory yields the time that a CAV is at a given position inside the control zone) by communicating with one another and with a *coordinator*, that is, a roadside unit that stores the planned time trajec-

ries of each CAV as it passes through the control zone. The distance from the entry of the control zone to the entry of the merging zone is S_c . Although it is not restrictive, we consider S_c to be the same for all entry points of the control zone. We also consider the merging zone to be a square of side S_m (see Figure 2). Note that S_c could be on the order of hundreds of meters, depending on the CAVs' communication range capability, while S_m is the length of a typical intersection. The CAVs crossing the intersection can also make a right turn of radius R_r and a left turn of radius R_l (see Figure 2).

The aforementioned values of the intersection's geometry are not restrictive in our modeling framework, and they are used only to determine the total distance traveled by each CAV inside the control zone. In our problem formulation, we assume that each CAV can communicate with other CAVs and the coordinator without any errors and delays. It is relatively straightforward to relax this assumption as long as the noise in the communication, measurements, and/or delays is bounded. We also assume that upon entering the control zone, the initial state of each CAV is feasible; that is, none of the speed and safety constraints are violated. This is a reasonable assumption since the CAVs are automated; therefore, there is no compelling reason for them to violate any of the constraints by the time they enter the control zone.

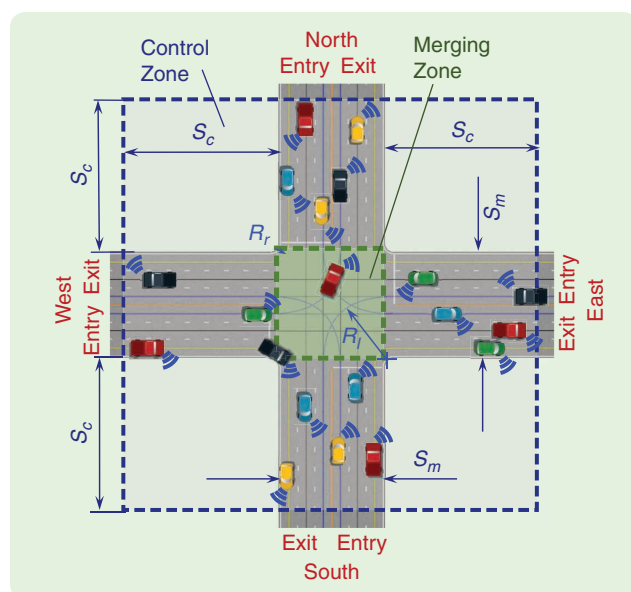


FIGURE 2 A signal-free intersection, with connected and automated vehicles.

We denote the set of CAVs in the control zone by the set $\mathcal{N}(t) = \{1, \dots, N(t)\}$, where $N(t) \in \mathbb{N}$ is the total number of CAVs at time $t \in \mathbb{R}_{\geq 0}$. In our framework, for each CAV $i \in \mathcal{N}(t)$, we seek to jointly minimize energy consumption and travel time. Upon entering the control zone, CAV i communicates with the coordinator and receives the time trajectory of all CAVs $j \in \mathcal{N}(t) \setminus \{i\}$. Next, CAV i computes the time t_i^f that it must exit the control zone while guaranteeing that its corresponding energy optimal time trajectory does not activate any of the state, control, and safety constraints. This trajectory is communicated back to the coordinator for subsequent CAVs to plan their trajectories with the same sequence as they enter the control zone. If two or more CAVs enter the control zone simultaneously, then the coordinator arbitrarily determines the sequence in which they receive information to plan their trajectories. Addressing the problem sequentially makes coordination among the CAVs tractable at the possible cost of selecting a suboptimal planning sequence. Finding the optimal sequence of decision making is a combinatorial problem, which is NP-hard [119]. In a recent paper, we reported how vehicles can dynamically change their decision-making sequence and replan to improve the throughput at an intersection [120] by relaxing the first-come, first-served decision making.

By enforcing the unconstrained energy optimal time trajectory that guarantees that none of the state, control, and safety constraints becomes active, we avoid the challenges associated with the real-time implementation of the constrained optimal control solution. In our analysis, we consider that each CAV $i \in \mathcal{N}(t)$ is governed by the following dynamics:

$$\dot{p}_i(t) = v_i(t), \quad \dot{v}_i(t) = u_i(t), \quad \dot{s}_i(t) = v_k(t) - v_i(t), \quad t \in [t_i^0, t_i^f] \quad (1)$$

where t_i^0 and t_i^f correspond to the times that CAV i enters and exits the control zone, respectively; $p_i(t) \in \mathcal{P}_i$ is the position of each CAV i from the entry to the exit of the control zone; $v_i(t) \in \mathcal{V}_i$ and $u_i(t) \in \mathcal{U}_i$ are the speed and acceleration/deceleration (control input), respectively, of each CAV i inside the control zone; $s_i(t) \in \mathcal{S}_i$ denotes the distance of CAV i from CAV k , which is physically located ahead of i ; and $v_k(t)$ is the speed of CAV k . The sets $\mathcal{P}_i, \mathcal{V}_i, \mathcal{U}_i$, and $\mathcal{S}_i, i \in \mathcal{N}(t)$ are complete and totally bounded subsets of \mathbb{R} .

In our framework, we impose the following constraints to ensure that the CAVs' control input and state remain within an admissible range:

$$u_{i,\min} \leq u_i(t) \leq u_{i,\max}, \quad 0 < v_{\min} \leq v_i(t) \leq v_{\max} \quad (2)$$

for all $t \in [t_i^0, t_i^f]$, where $u_{i,\min}, u_{i,\max}$ are the minimum and maximum control inputs and v_{\min}, v_{\max} are the minimum and maximum speed limit, respectively. To ensure that no rear-end collisions occur between two CAVs traveling in the same lane, we impose the rear-end safety constraint

$$s_i(t) = p_k(t) - \lambda_k - p_i(t) \geq \delta_i(t) = \gamma + \rho_i v_i(t) \quad (3)$$

where λ_k is the length of CAV k , γ is the standstill distance, and ρ_i is the minimum time headway that CAV i wishes to maintain with preceding CAV k .

Finally, let $j \in \mathcal{N}(t) \setminus \{i\}$ correspond to another CAV that has already entered the control zone and may have a lateral collision with CAV i . For example, suppose CAV i travels north-south and that CAV j travels east-west (see Figure 2). Then there is a *conflict point* where the paths of i and j intersect, and hence, a potential lateral collision might occur. We include all such conflict points in a finite set $\mathcal{O} \subset \mathbb{N}$, which is entirely determined by the geometry of the roads. Let p_i^n and p_j^n be the position of the conflict point $n \in \mathcal{O}$ along the paths of CAV i and j , respectively. CAV i can cross this conflict point either after or before CAV j . In the first case, we have

$$p_i^n - p_i(t) \geq \delta_i(t), \quad \text{for all } t \in [t_i^0, t_i^n] \quad (4)$$

where t_i^n is the known time that CAV j reaches at conflict point n , that is, position p_j^n . In the second case, we have

$$p_j^n - p_j(t) \geq \delta_j(t), \quad \text{for all } t \in [t_j^0, t_i^n] \quad (5)$$

where t_i^n is determined by the trajectory planned by CAV i .

Since $0 < v_{\min} \leq v_i(t)$, the position $p_i(t)$ is a strictly increasing function. Thus, the inverse $t_i(\cdot) = p_i^{-1}(\cdot)$ exists, and it is called the *time trajectory* of CAV i ; hence, we have $t_i^n = p_i^{-1}(p_i^n)$. The closed-form solution of the inverse function is derived in [47]. To guarantee lateral safety between CAV i and CAV j at a conflict point n , either (4) or (5) must be satisfied. Therefore, we impose the following lateral safety constraint on CAV i :

$$\min \left\{ \max_{t \in [t_i^0, t_i^n]} \{\delta_i(t) + p_i(t) - p_i^n\}, \max_{t \in [t_j^0, t_i^n]} \{\delta_j(t) + p_j(t) - p_j^n\} \right\} \leq 0. \quad (6)$$

When CAV $i \in \mathcal{N}(t)$ enters the control zone, it must determine the exit time t_i^f such that the resulting time trajectory does not activate any of (1)–(3) and (6). The unconstrained solution for CAV i is

$$\begin{aligned} u_i(t) &= 6a_i t + 2b_i, \quad v_i(t) = 3a_i t^2 + 2b_i t + c_i, \\ p_i(t) &= a_i t^3 + b_i t^2 + c_i t + d_i \end{aligned} \quad (7)$$

where a_i, b_i, c_i , and d_i are constants of integration. CAV i must also satisfy the boundary conditions $(p_i(t_i^0), v_i(t_i^0)) = (0, v_i^0)$ and $(p_i(t_i^f), u_i(t_i^f)) = (S_i, 0)$, where S_i is the known length of CAV i 's path in the control zone. For details on deriving the unconstrained solution, see "Unconstrained Optimal Control and Boundary Conditions."

There are five unknown variables that determine the optimal time trajectory of CAV i , four constants of integration from (7), and the unknown exit time t_i^f . Without a loss of generality, letting $t_i^0 = 0$ implies that $p_i(t_i^0) = d_i = 0$ and $v_i(t_i^0) = c_i = v_i^0$, while $u_i(t_i^f) = 0$ yields $a_i = -b_i/3t_i^f$, and

$p_i(t_i^f) = S_i$ gives $b_i = 3(S_i - v_i^0 t_i^f) / 2(t_i^f)^2$. Furthermore, t_i^f takes a value from a compact set, $[t_i^f, \bar{t}_i^f]$. See "Derivation of Bounds for Feasible Exit Time" for more details on the derivation t_i^f and \bar{t}_i^f based on the speed and control constraints and boundary conditions.

This leads to the optimization problem

$$\min_{t_i^f \in [t_i^f, \bar{t}_i^f]} t_i^f \quad (8)$$

subject to: rear-end safety (3); lateral safety (6); dynamics (7);

$$d_i = 0, \quad c_i = v_i^0, \quad a_i = -\frac{b_i}{3t_i^f}, \quad b_i = \frac{2(S_i - v_i^0 t_i^f)}{2(t_i^f)^2}.$$

The value of t_i^f guarantees that an unconstrained trajectory satisfies all the state, control, and safety constraints as well as the boundary conditions [47]. In practice, for each CAV $j \in \mathcal{N}(t)$, the coordinator stores the optimal exit time t_j^f and the corresponding coefficients a_j, b_j, c_j , and d_j . It has been shown [47] that there is no duality gap in (8). Therefore, the optimal solution can be derived in real time.

Each time a CAV i enters the control zone, it communicates with the coordinator and gets access to the time trajectories of all CAVs that are inside the control zone to derive its optimal exit time t_i^f from (8). Then, CAV i transmits its four coefficients and t_i^f back to the coordinator. In

the following section, we present a brief tutorial on applying our control framework to a multilane roundabout scenario, and we discuss several important insights that come from running scaled experiments.

TUTORIAL: ROUNDABOUT CASE STUDY

To illustrate the implementation of our framework, we performed experiments in one of the two multilane roundabouts of IDS³C (see Figure 3), using three CAVs per path. Figure 3 shows three paths with three conflict points that have a potential for lateral collisions, which we denote as lateral nodes. The length of the control zone for each path is 5.3, 5.8, and 3.8 m (132.5, 145, and 95 m scaled), respectively. The CAVs initially operate with an intelligent driver model controller [121] and switch to our control framework when entering the control zone. Each CAV then determines its time trajectory by solving (8) numerically. The CAVs follow this trajectory through the control zone. Upon exiting the control zone, they revert to the intelligent driver model and loop back around toward the control zone entrance.

For the experiments, we used the following parameters: $v_{\max} = 0.5$ m/s (28 mi/h at full scale), $v_{\min} = 0.15$ m/s (8.4 mi/h at full scale), $u_{\max} = 0.45$ m/s² (11 m/s² at full scale), and $u_{\min} = -u_{\max}$. To ensure safety, we selected

Unconstrained Optimal Control and Boundary Conditions

Let t_i^f be the specified exit time of connected and automated vehicle (CAV) i from the control zone. To minimize the energy consumption of i inside the control zone, we minimize transient engine operation through the L^2 norm of the control input $u_i(t)$ over the interval $[t_i^0, t_i^f]$, which is known to have a direct benefit in fuel consumption and emissions in conventional vehicles [S4], [S5]. Namely, CAV i minimizes the following cost function:

$$J_i(u_i(t), t_i^f) = \frac{1}{2} \int_{t_i^0}^{t_i^f} u_i(t)^2 dt. \quad (S1)$$

For each CAV i in the control zone, the unconstrained Hamiltonian is

$$H_i(t, p_i(t), v_i(t), u_i(t)) = \frac{1}{2} u_i(t)^2 + \lambda_i^p v_i(t) + \lambda_i^v u_i(t) \quad (S2)$$

where λ_i^p and λ_i^v are costates corresponding to the position and speed of the CAV, respectively. The Euler–Lagrange optimality equations are

$$\dot{\lambda}_i^p = -\frac{\partial H_i}{\partial p_i} = 0, \quad \dot{\lambda}_i^v = -\frac{\partial H_i}{\partial v_i} = -\lambda_i^p \quad (S3)$$

$$\frac{\partial H_i}{\partial u_i} = u_i + \lambda_i^v = 0. \quad (S4)$$

Since the speed of CAV i is not specified at the terminal time t_i^f , then [S1]

$$\lambda_i^v(t_i^f) = 0. \quad (S5)$$

Applying the Euler–Lagrange optimality conditions (S3) and (S4) to the Hamiltonian (S2) yields $u_i^*(t) = -\lambda_i^{v*} = a_i t + b_i$, where a_i and b_i are constants of integration. By integrating the control input, we can find the optimal position and speed trajectories as $p_i(t) = 1/6 a_i t^3 + 1/2 b_i t^2 + c_i t + d_i$ and $v_i(t) = 1/2 a_i t^2 + b_i t + c_i$, where a_i, b_i, c_i , and d_i are constants of integration, which are found by substituting the boundary conditions. The boundary conditions for any CAV i are $p_i(t_i^0) = p_i^0$, $v_i(t_i^0) = v_i^0$, $p_i(t_i^f) = p_i^f$, and $u_i(t_i^f) = 0$, where p_i is known at t_i^0 and t_i^f by the geometry of the road and v_i^0 is the speed at which the CAV enters the control zone. The final boundary condition, $u_i(t_i^f) = 0$, arises from substituting (S5) into (S4) at t_i^f ; that is, $u_i(t_i^f) + \lambda_i^v(t_i^f) = 0$, which implies $u_i(t_i^f) = 0$.

REFERENCES

- [S4] A. A. Malikopoulos, P. Y. Papalambros, and D. N. Assanis, "Online identification and stochastic control for autonomous internal combustion engines," *Trans. ASME, J. Dyn. Syst. Meas. Control*, vol. 132, no. 2, pp. 024504–024504, 2010, doi: 10.1115/1.4000819.
- [S5] A. A. Malikopoulos, D. N. Assanis, and P. Y. Papalambros, "Optimal engine calibration for individual driving styles," SAE International, Warrendale, PA, USA, SAE Tech. Paper 2008-01-1367, 2008.

Derivation of Bounds for Feasible Exit Time

The unconstrained optimal trajectory of connected and automated vehicle (CAV) $i \in \mathcal{N}(t)$ takes the form

$$u_i(t) = 6a_it + 2b_i \quad (S6)$$

$$v_i(t) = 3a_it^2 + 2b_it + c_i \quad (S7)$$

$$\rho_i(t) = a_it^3 + b_it^2 + c_it + d_i \quad (S8)$$

where $a_i, b_i, c_i,$ and d_i are constants of integration, which are found by using the boundary conditions. We derive the upper and lower bounds on the exit time of the control zone for a CAV $i \in \mathcal{N}(t)$, using the speed and control constraints by exploiting two properties of the optimal trajectory. Since the optimal control input is linear and satisfies $u_i(t_i^0) = 0$, it must be zero, strictly decreasing, or strictly increasing. In all three cases, $u_i(t)$ achieves its extreme at t_i^0 . Therefore, satisfying $u_{\min} \leq u_i(t_i^0) \leq u_{\max}$ is a necessary and sufficient condition to guarantee constraint satisfaction. Likewise, the speed of CAV i starts at $v_i(t_i^0) = v_i^0 \in [v_{\min}, v_{\max}]$ and must be constant, strictly increasing, or strictly decreasing inside the control zone. In all three cases, $v_i(t)$ takes its extreme value at t_i^f , and thus, satisfying $v_{\min} \leq v_i(t_i^f) \leq v_{\max}$ is a necessary and sufficient condition to guarantee constraint satisfaction.

Next, without a loss of generality, let $t_i^0 = 0$ and $\rho_i^0 = 0$. This implies $\rho_i(t_i^0) = d_i = 0$ and $v_i(t_i^0) = c_i = v_i^0$, while $u_i(t_i^0) = 0$ implies

$$a_i = \frac{-b_i}{3t_i^f} \quad (S9)$$

and $\rho_i(t_i^f) = S_i$ yields

$$b_i = \frac{3(S_i - v_i^0 t_i^f)}{2(t_i^f)^2}. \quad (S10)$$

To compute the lower bound on the exit time of the control zone for CAV i , t_i^f , there are two cases to consider.

CASE L1

CAV i achieves its maximum control input at the entry of the control zone; that is, $u_i(t_i^0) = u_{\max}$. In this case, evaluating (S6) at $t_i^0 = 0$ yields

$$u_i(t) = 2b_i = u_{\max}. \quad (S11)$$

Substituting (S10) into (S11) and solving for t_i^f yields the quadratic equation $u_{\max} t_i^f + 3v_i^0 t_i^f - 3S_i = 0$, which has two real roots with opposite signs since $t_{i,1}^f t_{i,2}^f = -3S_i/u_{\max} < 0$. Thus, $t_{i,U_{\max}}^f > 0$ is $t_{i,U_{\max}}^f = \sqrt{9v_i^0 + 12S_i u_{\max}} - 3v_i^0 / 2u_{\max}$.

CASE L2

CAV i achieves its maximum speed at the end of the control zone; that is, $v_i(t_i^f) = v_{\max}$. For this case, by (S7),

$$v_i(t_i^f) = 3a_i t_i^f + 2b_i t_i^f + v_i^0 = v_{\max}. \quad (S12)$$

Substituting (S9) and (S10) into (S12) yields

$$\begin{aligned} v_i(t_i^f) &= 3\left(\frac{-b_i}{3t_i^f}\right)t_i^f + 2b_i t_i^f + v_i^0 \\ &= b_i t_i^f + v_i^0 = \frac{3(S_i - v_i^0 t_i^f)}{2t_i^f} + v_i^0 = v_{\max} \end{aligned} \quad (S13)$$

which simplifies to $t_{i,v_{\max}}^f = 3S_i/v_i^0 + 2v_{\max}$. Thus, our lower bound on t_i^f is given by $t_i^f = \min\{t_{i,U_{\max}}^f, t_{i,v_{\max}}^f\}$. The upper bound for t_i^f can be derived following similar steps for the lower bound and can be broken into two cases.

CASE U1

CAV i achieves its minimum control input at the entry of the control zone; that is, $u_i(t_i^0) = u_{\min}$. This implies $u_{\min} t_i^f + 3v_i^0 t_i^f - 3S_i = 0$, which has two positive roots, as $t_{i,1}^f t_{i,2}^f = \frac{-3S_i}{u_{\min}} > 0$, from which we select the smaller one,

$$t_{i,U_{\min}}^f = \frac{\sqrt{9v_i^0 + 12S_i u_{\min}} - 3v_i^0}{2u_{\min}} \quad (S14)$$

since the speed of the vehicle should be always greater than zero. Note that when $9v_i^0 + 12S_i u_{\min} < 0$, there is no real value of t_i^f that satisfies all the boundary conditions simultaneously, and therefore, the constraint $u(t_i^0) = u_{\min}$ can never become active if (S14) is complex. In that case, the upper bound must be given by Case U2.

CASE U2

CAV i achieves its minimum speed at the entry of the control zone; that is, $v_i(t_i^0) = v_{\min}$. Evaluating (S7) at t_i^0 yields $v_i(t_i^0) = 3a_i t_i^0 + 2b_i t_i^0 + v_i^0 = v_{\min}$, in which substituting (S9) and (S10) yields

$$v_i(t_i^0) = 3\left(\frac{-b_i}{3t_i^0}\right)t_i^0 + 2b_i t_i^0 + v_i^0 = b_i t_i^0 + v_i^0 = \frac{3(S_i - v_i^0 t_i^0)}{2t_i^0} + v_i^0 = v_{\min} \quad (S15)$$

which simplifies to $t_{i,v_{\min}}^f = 3S_i/v_i^0 + 2v_{\min}$. Thus, the upper bound on the exit time for CAV i is

$$t_i^f = \begin{cases} t_{i,v_{\min}}^f, & \text{if } 9v_i^0 + 12S_i u_{i,\min} < 0, \\ \max\{t_{i,U_{\min}}^f, t_{i,v_{\min}}^f\}, & \text{otherwise} \end{cases} \quad (S16)$$

where $t_{i,v_{\min}}^f = 3S_i/v_i^0 + 2v_{\min}$ and $t_{i,U_{\min}}^f = \sqrt{9v_i^0 + 12S_i u_{\min}} - 3v_i^0 / 2u_{\min}$.

a time gap of 1 s and a minimum standstill distance of 0.07 m (approximately one car length). Our framework yields an average computation time of 2.14 ms, with a maximum of 3.4 ms when a CAV plans its trajectory. To quantify the effect of noise and disturbances acting on the system, we repeated the experiment five times. Furthermore, we precisely timed the release of the CAVs into the roundabout such that lateral collisions would occur without intervention. Videos of the roundabout experiment can be found at <https://sites.google.com/view/ud-ids-lab/csm>.

Minimum and average speed and travel time results for the five experiments are summarized in Table 1. Note that the minimum speed of all CAVs is 0.12 m/s (7 mi/h at full scale) across all experiments using our control framework, which demonstrates that stop-and-go driving has been completely eliminated. Additionally, the average speed of the CAVs is 0.42 m/s (24 mi/h at full scale), which implies that most CAVs travel near $v_{max} = 0.5$ m/s. The error between the desired and actual exit time varies

between 2% and 4%, which stems from the tracking error in the CAVs' low-level controller.

The exit time values for each CAV are visualized in Figure 4, showing the variation between the simulated and actual behavior of each CAV. The gray bars represent the feasible space of t_i^f , the wide black bars correspond to the planned value of t_i^f , and the thin red bars show the actual value of t_i^f achieved by each CAV. This effect of the tracking error is visible in Table 1, where the minimum achieved speed is slightly lower than the minimum speed imposed on the reference trajectory. Figure 4 also demonstrates how some scenarios can lead to a very small feasible space, that is, an exit time near the maximum. This can be seen in vehicles 17, 18, and 27. This motivates the introduction of a regularization zone upstream, which could influence the initial state of each CAV in the control zone to enlarge its feasible space.

Finally, the average, maximum, and minimum speeds for each CAV across all experiments are given in Figure 5. The subfigures correspond to a single path (see Figure 3) and consider 15 CAVs (three CAVs per path over five experiments). The CAVs' positions are taken directly from Vicon and numerically derived using a first-order method. From Figure 5, the average speed for the CAVs on each path is very close to constant. Path 1 shows the most variance, which is due to the distance between collision nodes 2 and 3 on path 1 (see Figure 3). For a CAV $i \in \mathcal{N}(t)$ that is traveling along path 1 to reduce its arrival time at node 2, it must make a proportionally larger reduction in the value of t_i^f . This is a side effect of enforcing the unconstrained trajectory on each CAV over the entire control zone.

The entrance to the control zone along path 3 follows a sharp right turn. This results in relatively lower average speed in Figure 5(c), as the dynamics of the CAVs reduce

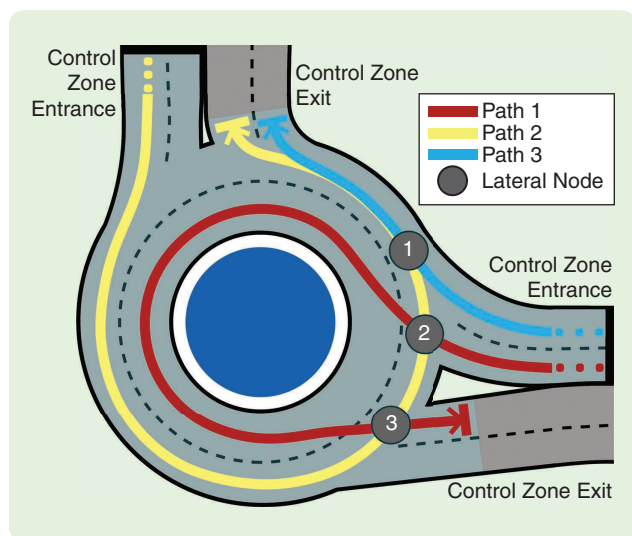


FIGURE 3 The roundabout scenario. The highlighted control zone continues upstream from the roundabout at both entrances.

TABLE 1 The minimum and average speed and travel time results for the five experiments. The root-mean-square error (RMSE) of the actual exit time compared to the desired exit time from the control zone averaged over all connected and automated vehicles in each experiment is provided.

Experiment	v_{min} (m/s)	v_{avg} (m/s)	Travel Time RMSE
1	0.16	0.41	2.71%
2	0.27	0.45	1.54%
3	0.18	0.41	4.03%
4	0.12	0.43	1.92%
5	0.21	0.42	1.38%

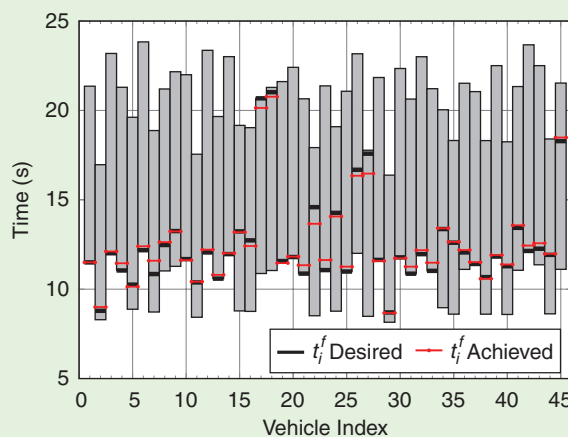
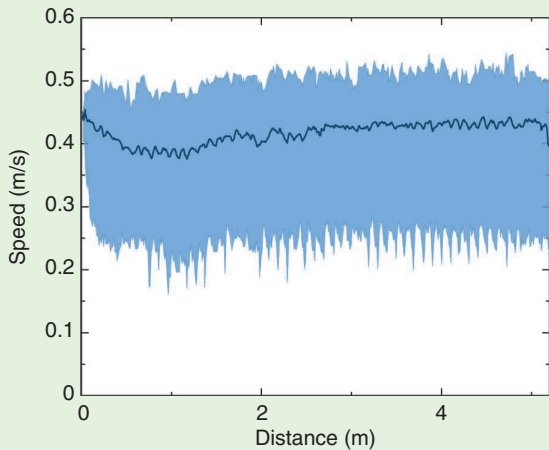
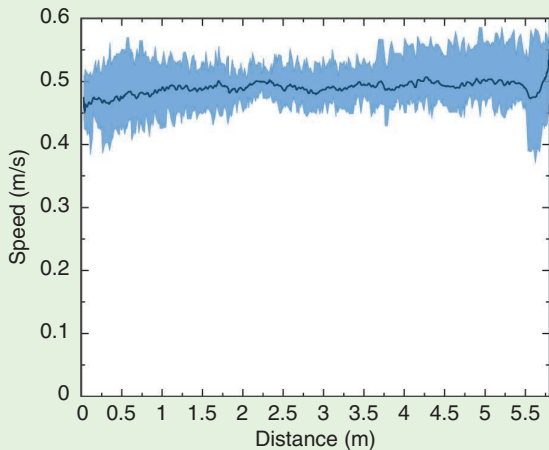


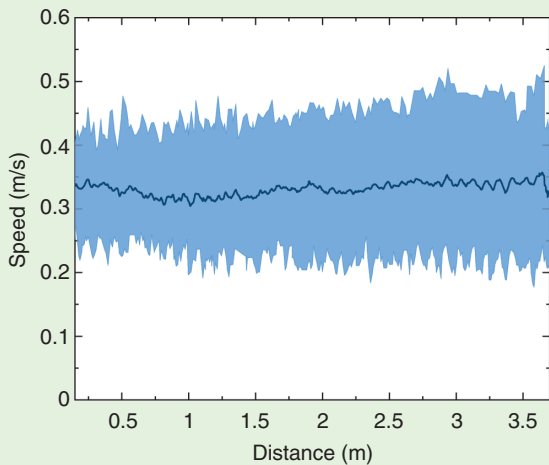
FIGURE 4 The planned and achieved exit time for each vehicle over all experiments. The gray bars show the range of admissible t_i^f from the state and control constraints. Every nine vehicles correspond to a single experiment; they are sorted in ascending order by their departure time from the control zone.



(a)



(b)



(c)

Speed Range — Speed Average

FIGURE 5 The speed range and average for all connected and automated vehicles on (a) path 1, (b) path 2, and (c) path 3 across all experiments in the multilane roundabout.

their speed while turning, causing them to enter the control zone at a lower initial speed. Finally, there are instances in Figure 5(b) where the maximum vehicle speed surpasses the speed limit. This is a result of stochasticity in the vehicle dynamics and sensing equipment as well as environmental disturbances on the deterministic controller. This analysis has motivated the development of an enhanced framework for CAV trajectory generation that accounts for noise, disturbances [120], communication delay [122], and low-level tracking errors [62], [117]. Next, we present a high-level overview and application of our control framework in a full transportation corridor in IDS³C.

TRANSPORTATION CORRIDOR

In this section, we apply our control framework in a transportation corridor in IDS³C, using 15 CAVs. The corridor is presented in Figure 6, where three ego CAVs are released along the red path (starting in the northeast of IDS³C) and travel through a roundabout, an intersection, and a merging roadway. In each traffic scenario, we release three additional CAVs per path (as indicated in Figure 6) to create congestion. The traffic scenarios were specifically selected so that upon entering the control zone, each CAV would have approximately 3 m (75 m scaled) to adjust its speed before reaching a conflict point. This also allowed us to consider each coordinator and control zone independently, as the control zone length was sufficiently long to neglect the influence of another upstream control zone.

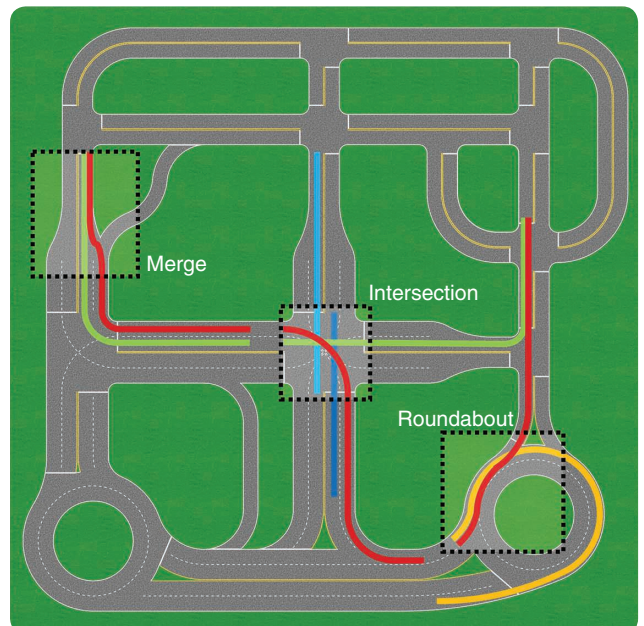


FIGURE 6 The corridor experiment, where the ego connected and automated vehicles (the red path) must navigate a roundabout, intersection, and merging roadway. The paths are colored only where they pass through a control zone, and the segments belonging to the same path have a shared color.

In the baseline case, we replaced the roundabout and merging zone coordinators with yield signs. In both scenarios, the merging vehicles yield to any vehicle within 0.4 m of the merging zone (10 m scaled; approximately four car lengths). To manage the intersection in the baseline case, we implemented a four-way stop with a first-in, first-out queue. Namely, whenever a vehicle enters a line segment leading up to the intersection, it is added to the queue. When the merging zone contains no vehicles, if the front vehicle has come to a complete stop, it is removed from the

queue and allowed to pass through the merging zone. We have taken this approach to the intersection to avoid any bias that may be introduced into our results by the timing of a traffic light.

Finally, to ensure a fair comparison, we set the speed limit for the entire city to 0.5 m/s (approximately 30 mi/h scaled) in both tests. In our framework, we impose a maximum speed of 0.3 m/s (approximately 15 mi/h scaled) outside of the control zone. This ensures that the vehicles enter the control zone at a speed lower than v_{max} and gives them the opportunity to accelerate through the control zone. Figure 7 shows that despite the apparent advantage of the baseline case's higher speed limit, the ego CAVs maintain a higher average speed in the optimal control case, and stop-and-go driving has been completely eliminated. Furthermore, Figure 8 demonstrates that the ego CAVs do not activate any safety constraints throughout the experiment. Additional videos and figures of the experiment can be found at <https://sites.google.com/view/ud-ids-lab/csm>.

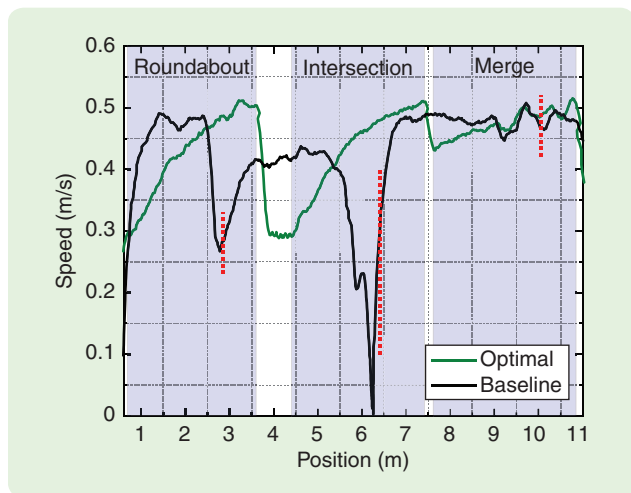


FIGURE 7 The speed-versus-position graph for the front ego vehicles in the optimal control and baseline cases. Blue-highlighted areas are within each of the control zones in the optimal case, and the vertical dashed lines correspond to the location of stop and yield signs in the baseline case.

CONCLUDING REMARKS

In this article, we introduced the IDS³C, a research and educational robotic scaled (1:25) testbed capable of safely validating control approaches beyond simulation in applications related to emerging mobility systems. This testbed can help us prove new emerging mobility concepts and understand the implications of errors/delays in vehicle-to-vehicle and vehicle-to-infrastructure communication. IDS³C can help us develop and implement control algorithms for coordinating CAVs in different traffic scenarios, such as intersections, merging roadways, speed reduction zones, roundabouts, and transportation corridors.

On the educational and outreach fronts, IDS³C has been used to 1) train and educate graduate students by exposing them to a balanced mix of theory and practice, 2) integrate research outcomes into existing courses, 3) involve undergraduate students in research, 4) create interactive educational demos, and 5) reach out to high-school students. IDS³C has been a research and educational catalyst for motivating interest in undergraduate and high-school students in science, technology, engineering, and mathematics.

We also provided an overview of a control framework for coordinating CAVs. We demonstrated its effectiveness in IDS³C in a multilane roundabout, using nine CAVs, and in a corridor consisting of a roundabout, an intersection, and a merging roadway, using 15 CAVs. Ongoing research considers enhancing the framework by incorporating uncertainty originated from the vehicle surroundings [62], [117] and the effects of errors and delays in vehicle-to-vehicle and vehicle-to-infrastructure communication [122]. Another direction of current research considers how to operate the CAVs in a way to indirectly control

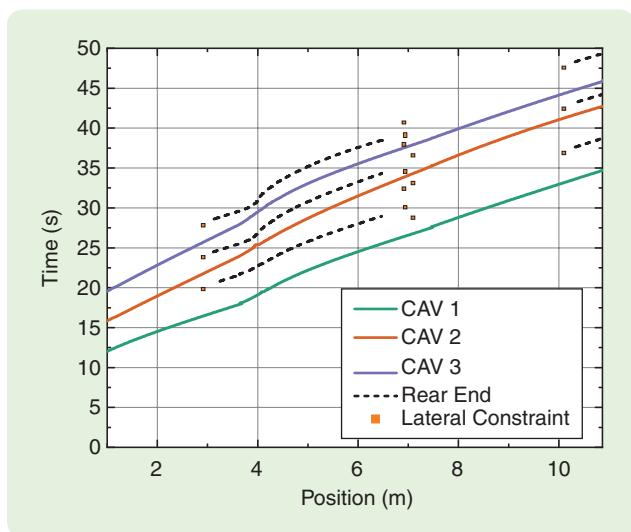


FIGURE 8 The time-versus-position graph for the ego connected and automated vehicles (CAVs) in the optimal control case. Solid lines correspond to the CAV trajectories, dashed lines correspond to CAVs that merge onto the ego path, and orange boxes correspond to time intervals when a lateral conflict point is occupied by another CAV.

human-driven vehicles and force them to form platoons led by CAVs [20], [123].

ACKNOWLEDGMENT

This work was supported in part by the National Science Foundation under Grant CMMI-2219761. This support is gratefully acknowledged. The authors would like to also acknowledge Raymond Zayas and Amanda Kelly for their effort in designing, building, testing, and maintaining the newest generation of CAVs used in this article. The authors would also like to thank Joel Diaz Goenaga for creating animations of the scaled CAV exploded view.

AUTHOR INFORMATION

Behdad Chalaki received the B.S. degree in mechanical engineering from the University of Tehran, Iran, in 2017. He received the M.S. degree from the Department of Mechanical Engineering, University of Delaware, Newark, DE 19716 USA, in 2021, where he is currently a Ph.D. candidate in the Information and Decision Science Laboratory, Department of Mechanical Engineering. His primary research interests lie at the intersections of decentralized optimal control, statistics, and machine learning, with an emphasis on transportation networks. In particular, he is motivated by problems related to improving traffic efficiency and safety in smart cities by using optimization techniques. He is a Student Member of IEEE, the Society of Industrial and Applied Mathematics, the American Society of Mechanical Engineers, and the American Association for the Advancement of Science.

Logan E. Beaver received the B.S. degree in mechanical engineering from the Milwaukee School of Engineering, Wisconsin, USA, in 2015 and the M.S. degree in mechanical engineering from Marquette University, Milwaukee, in 2017. He is currently a Ph.D. candidate in the Information and Decision Science Laboratory, Department of Mechanical Engineering, University of Delaware, Newark, DE 19716 USA. His research focuses on the detection, stabilization, and control of emergent behavior in multiagent and swarm systems. He is a Student Member of IEEE, the Society of Industrial and Applied Mathematics, the American Society of Mechanical Engineers, and the American Association for the Advancement of Science.

A.M. Ishtiaque Mahbub received the B.S. degree in mechanical engineering from the Bangladesh University of Engineering and Technology, Dhaka, in 2013; M.Sc. in computational mechanics from the University of Stuttgart, Germany, in 2016; and M.Sc. in mechanical engineering from the University of Delaware in 2021. He is currently pursuing a Ph.D. degree in mechanical engineering in the Information Decision Science Laboratory, University of Delaware, Newark, DE 19716 USA, under the supervision of Prof. Andreas A. Malikopoulos. His research interests include, but are not limited to, optimization and control, with an emphasis on applications related to connected

automated vehicles, hybrid electric vehicles, and intelligent transportation systems. He has conducted several internships at the National Renewable Energy Lab; Robert Bosch, in the United States and Germany; and Fraunhofer IPA. He is a Student Member of IEEE, the Society of Industrial and Applied Mathematics, and the Society of Automotive Engineers.

Heeseung Bang received the B.S. degree in mechanical engineering and the M.S. degree in electrical engineering from Inha University, Incheon, South Korea, in 2018 and 2020, respectively. He is currently a Ph.D. student in the Department of Mechanical Engineering, University of Delaware, Newark, DE 19716 USA. His research interests include the optimization and control of multiagent systems, with an emphasis on autonomous mobility-on-demand systems, future mobility systems, and smart cities. He is a Student Member of IEEE.

Andreas A. Malikopoulos (andreas@udel.edu) received the Diploma degree in mechanical engineering from the National Technical University of Athens, Greece, in 2000. He received the M.S. and Ph.D. degrees from the Department of Mechanical Engineering, University of Michigan, Ann Arbor, USA, in 2004 and 2008, respectively. He is the Terri Connor Kelly and John Kelly Career Development Associate Professor in the Department of Mechanical Engineering, University of Delaware (UD), Newark, DE 19716 USA, where he is the director of the Information and Decision Science Laboratory and the Sociotechnical Systems Center. Before he joined UD, he was the deputy director and lead of the Sustainable Mobility Theme of the Urban Dynamics Institute, Oak Ridge National Laboratory, and a senior researcher with General Motors Global Research and Development. His research interests span several fields, including the analysis, optimization, and control of cyber-physical systems; decentralized systems; stochastic scheduling and resource allocation problems; and learning in complex systems, with an emphasis on applications related to smart cities, emerging mobility systems, and sociotechnical systems. He was an associate editor of *IEEE Transactions on Intelligent Vehicles* and *IEEE Transactions on Intelligent Transportation Systems* from 2017 to 2020. He is currently an associate editor of *Automatica* and *IEEE Transactions on Automatic Control*. He is a Senior Member of IEEE, a member of the Society of Industrial and Applied Mathematics and the American Association for the Advancement of Science, and a fellow of the American Society of Mechanical Engineers.

REFERENCES

- [1] L. Zhao and A. A. Malikopoulos, "Enhanced mobility with connectivity and automation: A review of shared autonomous vehicle systems," *IEEE Intell. Transp. Syst. Mag.*, vol. 14, no. 1, pp. 87–102, Jan./Feb. 2022, doi: 10.1109/MITS.2019.2953526.
- [2] A. A. Malikopoulos, "A duality framework for stochastic optimal control of complex systems," *IEEE Trans. Autom. Control*, vol. 61, no. 10, pp. 2756–2765, Oct. 2016, doi: 10.1109/TAC.2015.2504518.
- [3] K. Spieser, K. Treleven, R. Zhang, E. Frazzoli, D. Morton, and M. Pavone, "Toward a systematic approach to the design and evaluation of

- automated mobility-on-demand systems: A case study in Singapore," in *Road Vehicle Automation*, G. Meyer and S. Beiker, Eds. Cham, Switzerland: Springer-Verlag, 2014, pp. 229–245.
- [4] J. Rios-Torres and A. A. Malikopoulos, "Impact of partial penetrations of connected and automated vehicles on fuel consumption and traffic flow," *IEEE Trans. Intell. Veh.*, vol. 3, no. 4, pp. 453–462, Dec. 2018, doi: 10.1109/TIV.2018.2873899.
- [5] L. Zhao, A. A. Malikopoulos, and J. Rios-Torres, "Optimal control of connected and automated vehicles at roundabouts: An investigation in a mixed-traffic environment," in *Proc. 15th IFAC Symp. Control Transp. Syst.*, 2018, pp. 73–78, doi: 10.1016/j.ifacol.2018.07.013.
- [6] Y. Zhang and C. G. Cassandras, "An impact study of integrating connected automated vehicles with conventional traffic," *Annu. Rev. Control*, vol. 48, pp. 347–356, Apr. 2019, doi: 10.1016/j.arcontrol.2019.04.009.
- [7] S. E. Shladover et al., "Automated vehicle control developments in the PATH program," *IEEE Trans. Veh. Technol.*, vol. 40, no. 1, pp. 114–130, Feb. 1991, doi: 10.1109/25.69979.
- [8] P. Varaiya, "Smart cars on smart roads: Problems of control," *IEEE Trans. Autom. Control*, vol. 38, no. 2, pp. 195–207, Feb. 1993, doi: 10.1109/9.250509.
- [9] R. Rajamani, H.-S. Tan, B. K. Law, and W.-B. Zhang, "Demonstration of integrated longitudinal and lateral control for the operation of automated vehicles in platoons," *IEEE Trans. Control Syst. Technol.*, vol. 8, no. 4, pp. 695–708, Jul. 2000, doi: 10.1109/87.852914.
- [10] S. Van De Hoef, K. H. Johansson, and D. V. Dimarogonas, "Fuel-efficient En route formation of truck platoons," *IEEE Trans. Intell. Transp. Syst.*, vol. 19, no. 1, pp. 102–112, Jan. 2018, doi: 10.1109/TITS.2017.2700021.
- [11] Z. Wang, G. Wu, P. Hao, K. Boriboonsomsin, and M. Barth, "Developing a platoon-wide eco-cooperative adaptive cruise control (CACC) system," in *Proc. 2017 IEEE Intell. Veh. Symp. (IV)*, pp. 1256–1261, doi: 10.1109/IVS.2017.7995884.
- [12] A. Johansson, E. Nekouei, K. H. Johansson, and J. Mårtensson, "Multi-fleet platoon matching: A game-theoretic approach," in *Proc. 2018 21st Int. Conf. Intell. Transp. Syst. (ITSC)*, pp. 2980–2985, doi: 10.1109/ITSC.2018.8569379.
- [13] S. Karbalaieali, O. A. Osman, and S. Ishak, "A dynamic adaptive algorithm for merging into platoons in connected automated environments," *IEEE Trans. Intell. Transp. Syst.*, vol. 21, no. 10, pp. 4111–4122, Oct. 2020, doi: 10.1109/TITS.2019.2938728.
- [14] S. Yao and B. Friedrich, "Managing connected and automated vehicles in mixed traffic by human-leading platooning strategy: A simulation study," in *Proc. 2019 IEEE Intell. Transp. Syst. Conf. (ITSC)*, pp. 3224–3229, doi: 10.1109/ITSC.2019.8917007.
- [15] X. Xiong, E. Xiao, and L. Jin, "Analysis of a stochastic model for coordinated platooning of heavy-duty vehicles," in *Proc. 2019 IEEE 58th Conf. Decis. Control (CDC)*, pp. 3170–3175, doi: 10.1109/CDC40024.2019.9029179.
- [16] N. Pourmohammad-Zia, F. Schulte, and R. R. Negenborn, "Platform-based platooning to connect two autonomous vehicle areas," in *Proc. 2020 IEEE 23rd Int. Conf. Intell. Transp. Syst. (ITSC)*, pp. 1–6, doi: 10.1109/ITSC45102.2020.9294689.
- [17] T. Ard, F. Ashtiani, A. Vahidi, and H. Borhan, "Optimizing gap tracking subject to dynamic losses via connected and anticipative MPC in truck platooning," in *Proc. 2020 Amer. Control Conf. (ACC)*, pp. 2300–2305, doi: 10.23919/ACC45564.2020.9147849.
- [18] S. Kumaravel, A. A. Malikopoulos, and R. Ayyagari, "Decentralized cooperative merging of platoons of connected and automated vehicles at highway on-ramps," in *Proc. 2021 Amer. Control Conf. (ACC)*, pp. 2055–2060, doi: 10.23919/ACC50511.2021.9483390.
- [19] S. Kumaravel, A. A. Malikopoulos, and R. Ayyagari, "Optimal coordination of platoons of connected and automated vehicles at signal-free intersections," *IEEE Trans. Intell. Veh.*, vol. 7, no. 2, pp. 186–197, Jun. 2022, doi: 10.1109/TIV.2021.3096993.
- [20] A. M. I. Mahbub and A. A. Malikopoulos, "A platoon formation framework in a mixed traffic environment," *IEEE Control Syst. Lett.*, vol. 6, pp. 1370–1375, 2022, doi: 10.1109/LCSYS.2021.3092188.
- [21] A. K. Bhoopalam, N. Agatz, and R. Zuidwijk, "Planning of truck platoons: A literature review and directions for future research," *Transp. Res. B, Methodol.*, vol. 107, pp. 212–228, Jan. 2018, doi: 10.1016/j.trb.2017.10.016.
- [22] A. M. Ishtiaque Mahbub and A. A. Malikopoulos, "Platoon formation in a mixed traffic environment: A model-agnostic optimal control approach," in *Proc. Amer. Control Conf.*, Oct. 2022, pp. 4746–4751, doi: 10.23919/ACC53348.2022.9867168.
- [23] M. Athans, "A unified approach to the vehicle-merging problem," *Transp. Res.*, vol. 3, no. 1, pp. 123–133, 1969, doi: 10.1016/0041-1647(69)90109-9.
- [24] W. Levine and M. Athans, "On the optimal error regulation of a string of moving vehicles," *IEEE Trans. Autom. Control*, vol. 11, no. 3, pp. 355–361, Jul. 1966, doi: 10.1109/TAC.1966.1098376.
- [25] K. Dresner and P. Stone, "A multiagent approach to autonomous intersection management," *J. Artif. Intell. Res.*, vol. 31, pp. 591–656, Mar. 2008, doi: 10.1613/jair.2502.
- [26] L. Makarem and D. Gillet, "Fluent coordination of autonomous vehicles at intersections," in *Proc. 2012 IEEE Int. Conf. Syst., Man, Cybern. (SMC)*, pp. 2557–2562, doi: 10.1109/ICSMC.2012.6378130.
- [27] J. Lee and B. Park, "Development and evaluation of a cooperative vehicle intersection control algorithm under the connected vehicles environment," *IEEE Trans. Intell. Transp. Syst.*, vol. 13, no. 1, pp. 81–90, Mar. 2012, doi: 10.1109/TITS.2011.2178836.
- [28] K.-D. Kim and P. Kumar, "An MPC-based approach to provable system-wide safety and liveness of autonomous ground traffic," *IEEE Trans. Autom. Control*, vol. 59, no. 12, pp. 3341–3356, Dec. 2014, doi: 10.1109/TAC.2014.2351911.
- [29] R. Azimi, G. Bhatia, R. R. Rajkumar, and P. Mudalige, "STIP: Spatio-temporal intersection protocols for autonomous vehicles," in *Proc. 2014 ACM/IEEE Int. Conf. Cyber-Phys. Syst. (ICCP)*, pp. 1–12, doi: 10.1109/IC-CP.2014.6843706.
- [30] W. Wu, J. Zhang, A. Luo, and J. Cao, "Distributed mutual exclusion algorithms for intersection traffic control," *IEEE Trans. Parallel Distrib. Syst.*, vol. 26, no. 1, pp. 65–74, Jan. 2015, doi: 10.1109/TPDS.2013.2297097.
- [31] A. Colombo and D. Del Vecchio, "Least restrictive supervisors for intersection collision avoidance: A scheduling approach," *IEEE Trans. Autom. Control*, vol. 60, no. 6, pp. 1515–1527, Jun. 2015, doi: 10.1109/TAC.2014.2381453.
- [32] M. A. S. Kamal, J.-i. Mura, T. Hayakawa, A. Ohata, and K. Aihara, "A vehicle-intersection coordination scheme for smooth flows of traffic without using traffic lights," *IEEE Trans. Intell. Transp. Syst.*, vol. 16, no. 3, pp. 1136–1147, Jun. 2015, doi: 10.1109/TITS.2014.2354380.
- [33] J. Gregoire, S. Bonnabel, and A. De La Fortelle, "Priority-based intersection management with kinodynamic constraints," in *Proc. 2014 Eur. Control Conf.*, pp. 2902–2907, doi: 10.1109/ECC.2014.6862377.
- [34] A. A. Malikopoulos, C. G. Cassandras, and Y. J. Zhang, "A decentralized energy-optimal control framework for connected automated vehicles at signal-free intersections," *Automatica*, vol. 93, pp. 244–256, Jul. 2018, doi: 10.1016/j.automatica.2018.03.056.
- [35] S. A. Fayazi and A. Vahidi, "Mixed-integer linear programming for optimal scheduling of autonomous vehicle intersection crossing," *IEEE Trans. Intell. Veh.*, vol. 3, no. 3, pp. 287–299, Sep. 2018, doi: 10.1109/TIV.2018.2843163.
- [36] R. Hult, M. Zanon, S. Gros, and P. Falcone, "Optimal coordination of automated vehicles at intersections: Theory and experiments," *IEEE Trans. Control Syst. Technol.*, vol. 27, no. 6, pp. 2510–2525, Nov. 2019, doi: 10.1109/TCST.2018.2871397.
- [37] H. Wei, L. Mashayekhy, and J. Papineau, "Intersection management for connected autonomous vehicles: A game theoretic framework," in *Proc. 2018 21st Int. Conf. Intell. Transp. Syst. (ITSC)*, pp. 583–588, doi: 10.1109/ITSC.2018.8569307.
- [38] Y. Bichiou and H. A. Rakha, "Developing an optimal intersection control system for automated connected vehicles," *IEEE Trans. Intell. Transp. Syst.*, vol. 20, no. 5, pp. 1908–1916, May 2019, doi: 10.1109/TITS.2018.2850335.
- [39] A. Mirheli, M. Tajalli, L. Hajibabai, and A. Hajbabaie, "A consensus-based distributed trajectory control in a signal-free intersection," *Transp. Res. C, Emerg. Technol.*, vol. 100, pp. 161–176, Mar. 2019, doi: 10.1016/j.trc.2019.01.004.
- [40] M. Kloock, P. Scheffe, S. Marquardt, J. Maczjewski, B. Alrifaaee, and S. Kowalewski, "Distributed model predictive intersection control of multiple vehicles," in *Proc. 2019 IEEE Intell. Transp. Syst. Conf. (ITSC)*, pp. 1735–1740, doi: 10.1109/ITSC.2019.8917117.
- [41] Y. Zhang and C. G. Cassandras, "Decentralized optimal control of connected automated vehicles at signal-free intersections including comfort-constrained turns and safety guarantees," *Automatica*, vol. 109, p. 108,563, Nov. 2019, doi: 10.1016/j.automatica.2019.108563.
- [42] A. A. Malikopoulos and L. Zhao, "Optimal path planning for connected and automated vehicles at urban intersections," in *Proc. 58th IEEE Conf. Decis. Control*, 2019, pp. 1261–1266, doi: 10.1109/CDC40024.2019.9030093.
- [43] A. A. Malikopoulos and L. Zhao, "A closed-form analytical solution for optimal coordination of connected and automated vehicles," in *Proc. 2019 Amer. Control Conf. (ACC)*, pp. 3599–3604, doi: 10.23919/ACC.2019.8814759.

- [44] R. Tian, N. Li, I. Kolmanovsky, Y. Yildiz, and A. R. Girard, "Game-theoretic modeling of traffic in unsignalized intersection network for autonomous vehicle control verification and validation," *IEEE Trans. Intell. Transp. Syst.*, vol. 23, no. 3, pp. 2211–2226, Mar. 2022, doi: 10.1109/TITS.2020.3035363.
- [45] X. Pan, B. Chen, S. A. Evangelou, and S. Timotheou, "Optimal motion control for connected and automated electric vehicles at signal-free intersections," in *Proc. 2020 59th IEEE Conf. Decis. Control (CDC)*, pp. 2831–2836, doi: 10.1109/CDC42340.2020.9304392.
- [46] H. Xu, C. G. Cassandras, L. Li, and Y. Zhang, "Comparison of cooperative driving strategies for CAVs at signal-free intersections," *IEEE Trans. Intell. Transp. Syst.*, vol. 23, no. 7, pp. 7614–7627, Jul. 2022, doi: 10.1109/TITS.2021.3071456.
- [47] A. A. Malikopoulos, L. E. Beaver, and I. V. Chremos, "Optimal time trajectory and coordination for connected and automated vehicles," *Automatica*, vol. 125, p. 109469, Mar. 2021, doi: 10.1016/j.automatica.2020.109469.
- [48] B. Chalaki and A. A. Malikopoulos, "A hysteretic q-learning coordination framework for emerging mobility systems in smart cities," in *Proc. 2021 Eur. Control Conf. (ECC)*, pp. 17–22, doi: 10.23919/ECC54610.2021.9655172.
- [49] H. Xu, Y. Zhang, L. Li, and W. Li, "Cooperative driving at unsignalized intersections using tree search," *IEEE Trans. Intell. Transp. Syst.*, vol. 21, no. 11, pp. 4563–4571, Nov. 2020, doi: 10.1109/TITS.2019.2940641.
- [50] M. A. Guney and I. A. Raptis, "Scheduling-based optimization for motion coordination of autonomous vehicles at multilane intersections," *J. Robot.*, vol. 2020, Mar. 2020, Art. no. 6217409, doi: 10.1155/2020/6217409.
- [51] K. Dresner and P. Stone, "Multiagent traffic management: A reservation-based intersection control mechanism," in *Proc. 3rd Int. Joint Conf. Auton. Agents Multiagents Syst.*, 2004, pp. 530–537.
- [52] A. de La Fortelle, "Analysis of reservation algorithms for cooperative planning at intersections," in *Proc. 13th Int. IEEE Conf. Intell. Transp. Syst.*, 2010, pp. 445–449, doi: 10.1109/ITSC.2010.5624978.
- [53] M. Hausknecht, T.-C. Au, and P. Stone, "Autonomous intersection management: Multi-intersection optimization," in *Proc. 2011 IEEE/RSJ Int. Conf. Intell. Robots Syst.*, pp. 4581–4586, doi: 10.1109/IROS.2011.6094668.
- [54] S. Huang, A. Sadek, and Y. Zhao, "Assessing the mobility and environmental benefits of reservation-based intelligent intersections using an integrated simulator," *IEEE Trans. Intell. Transp. Syst.*, vol. 13, no. 3, pp. 1201–1214, Sep. 2012, doi: 10.1109/TITS.2012.2186442.
- [55] Q. Jin, G. Wu, K. Boriboonsomsin, and M. Barth, "Multi-agent intersection management for connected vehicles using an optimal scheduling approach," in *Proc. 2012 Int. Conf. Connected Veh. Expo (ICCVe)*, pp. 185–190, doi: 10.1109/ICCVe.2012.41.
- [56] M. W. Levin, H. Fritz, and S. D. Boyles, "On optimizing reservation-based intersection controls," *IEEE Trans. Intell. Transp. Syst.*, vol. 18, no. 3, pp. 505–515, Mar. 2017, doi: 10.1109/TITS.2016.2574948.
- [57] Z. Du, B. HomChaudhuri, and P. Pisu, "Hierarchical distributed coordination strategy of connected and automated vehicles at multiple intersections," *J. Intell. Transp. Syst.*, vol. 22, no. 2, pp. 144–158, 2018, doi: 10.1080/15472450.2017.1407930.
- [58] F. Ashtiani, S. A. Fayazi, and A. Vahidi, "Multi-intersection traffic management for autonomous vehicles via distributed mixed integer linear programming," in *Proc. 2018 Annu. Amer. Control Conf. (ACC)*, pp. 6341–6346, doi: 10.23919/ACC.2018.8431656.
- [59] C. Yu, Y. Feng, H. X. Liu, W. Ma, and X. Yang, "Corridor level cooperative trajectory optimization with connected and automated vehicles," *Transp. Res. C, Emerg. Technol.*, vol. 105, pp. 405–421, Aug. 2019, doi: 10.1016/j.trc.2019.06.002.
- [60] A. M. I. Mahbub, L. Zhao, D. Assanis, and A. A. Malikopoulos, "Energy-optimal coordination of connected and automated vehicles at multiple intersections," in *Proc. 2019 Amer. Control Conf.*, pp. 2664–2669, doi: 10.23919/ACC.2019.8814877.
- [61] B. Chalaki and A. A. Malikopoulos, "Time-optimal coordination for connected and automated vehicles at adjacent intersections," *IEEE Trans. Intell. Transp. Syst.*, vol. 23, no. 8, pp. 13330–13345, Aug. 2022, doi: 10.1109/TITS.2021.3123479.
- [62] B. Chalaki and A. A. Malikopoulos, "Optimal control of connected and automated vehicles at multiple adjacent intersections," *IEEE Trans. Control Syst. Technol.*, vol. 30, no. 3, pp. 972–984, May 2022, doi: 10.1109/TCST.2021.3082306.
- [63] B. Chalaki and A. A. Malikopoulos, "An optimal coordination framework for connected and automated vehicles in two interconnected intersections," in *Proc. 2019 IEEE Conf. Control Technol. Appl. (CCTA)*, pp. 888–893, doi: 10.1109/CCTA.2019.8920448.
- [64] M. Rodriguez and H. K. Fathy, "Distributed Kuramoto self-synchronization of vehicle speed trajectories in traffic networks," *IEEE Trans. Intell. Transp. Syst.*, vol. 23, no. 7, pp. 6786–6796, Jul. 2022, doi: 10.1109/TITS.2021.3062178.
- [65] H. Pei, Y. Zhang, Q. Tao, S. Feng, and L. Li, "Distributed cooperative driving in multi-intersection road networks," *IEEE Trans. Veh. Technol.*, vol. 70, no. 6, pp. 5390–5403, Jun. 2021, doi: 10.1109/TVT.2021.3079272.
- [66] L. Zhao, A. M. I. Mahbub, and A. A. Malikopoulos, "Optimal vehicle dynamics and powertrain control for connected and automated vehicles," in *Proc. 2019 IEEE Conf. Control Technol. Appl. (CCTA)*, pp. 33–38, doi: 10.1109/CCTA.2019.8920531.
- [67] J. Rios-Torres and A. A. Malikopoulos, "Automated and cooperative vehicle merging at highway on-ramps," *IEEE Trans. Intell. Transp. Syst.*, vol. 18, no. 4, pp. 780–789, Apr. 2017, doi: 10.1109/TITS.2016.2587582.
- [68] I. A. Ntousakis, I. K. Nikolos, and M. Papageorgiou, "Optimal vehicle trajectory planning in the context of cooperative merging on highways," *Transp. Res. C, Emerg. Technol.*, vol. 71, pp. 464–488, Oct. 2016, doi: 10.1016/j.trc.2016.08.007.
- [69] F. Belletti, D. Haziza, G. Gomes, and A. M. Bayen, "Expert level control of ramp metering based on multi-task deep reinforcement learning," *IEEE Trans. Intell. Transp. Syst.*, vol. 19, no. 4, pp. 1198–1207, Apr. 2018, doi: 10.1109/TITS.2017.2725912.
- [70] Y. Ito, M. A. S. Kamal, T. Yoshimura, and S.-i. Azuma, "Coordination of connected vehicles on merging roads using pseudo-perturbation-based broadcast control," *IEEE Trans. Intell. Transp. Syst.*, vol. 20, no. 9, pp. 3496–3512, Sep. 2019, doi: 10.1109/TITS.2018.2876905.
- [71] A. Stager, L. Bhan, A. A. Malikopoulos, and L. Zhao, "A scaled smart city for experimental validation of connected and automated vehicles," in *Proc. 15th IFAC Symp. Control Transp. Syst.*, 2018, pp. 130–135, doi: 10.1016/j.ifacol.2018.07.022.
- [72] S. Jing, F. Hui, X. Zhao, J. Rios-Torres, and A. J. Khattak, "Cooperative game approach to optimal merging sequence and on-ramp merging control of connected and automated vehicles," *IEEE Trans. Intell. Transp. Syst.*, vol. 20, no. 11, pp. 4234–4244, Nov. 2019, doi: 10.1109/TITS.2019.2925871.
- [73] J. Ding, L. Li, H. Peng, and Y. Zhang, "A rule-based cooperative merging strategy for connected and automated vehicles," *IEEE Trans. Intell. Transp. Syst.*, vol. 21, no. 8, pp. 3436–3446, Aug. 2020, doi: 10.1109/TITS.2019.2928969.
- [74] W. Xiao, C. G. Cassandras, and C. Belta, "Decentralized optimal control in multi-lane merging for connected and automated vehicles," in *Proc. 2020 IEEE 23rd Int. Conf. Intell. Transp. Syst. (ITSC)*, pp. 1–6, doi: 10.1109/ITSC45102.2020.9294469.
- [75] X. Liao et al., "Cooperative ramp merging design and field implementation: A digital twin approach based on vehicle-to-cloud communication," *IEEE Trans. Intell. Transp. Syst.*, vol. 23, no. 5, pp. 4490–4500, May 2022, doi: 10.1109/TITS.2020.3045123.
- [76] I. H. Zohdy and H. A. Rakha, "Enhancing roundabout operations via vehicle connectivity," *Transp. Res. Rec.*, vol. 2381, no. 1, pp. 91–100, 2013, doi: 10.3141/2381-11.
- [77] E. Debada, L. Makarem, and D. Gillet, "Autonomous coordination of heterogeneous vehicles at roundabouts," in *Proc. 2016 IEEE 19th Int. Conf. Intell. Transp. Syst. (ITSC)*, pp. 1489–1495, doi: 10.1109/ITSC.2016.7795754.
- [78] A. Bakibillah et al., "The optimal coordination of connected and automated vehicles at roundabouts," in *Proc. 2019 58th Annu. Conf. Soc. Instrum. Control Eng. Japan (SICE)*, pp. 1392–1397, doi: 10.23919/SICE.2019.8860072.
- [79] B. Chalaki, L. E. Beaver, and A. A. Malikopoulos, "Experimental validation of a real-time optimal controller for coordination of CAVs in a multi-lane roundabout," in *Proc. 31st IEEE Intell. Veh. Symp. (IV)*, 2020, pp. 775–780, doi: 10.1109/IV47402.2020.9304531.
- [80] K. Xu, C. G. Cassandras, and W. Xiao, "Decentralized time and energy-optimal control of connected and automated vehicles in a roundabout," 2021, *arXiv:2104.06242*.
- [81] K. Jang et al., "Simulation to scaled city: Zero-shot policy transfer for traffic control via autonomous vehicles," in *Proc. 10th ACM/IEEE Int. Conf. Cyber-Phys. Syst.*, 2019, pp. 291–300, doi: 10.1145/3302509.3313784.
- [82] B. Chalaki et al., "Zero-shot autonomous vehicle policy transfer: From simulation to real-world via adversarial learning," in *Proc. IEEE 16th Int. Conf. Control Autom. (ICCA)*, 2020, pp. 35–40, doi: 10.1109/ICCA51439.2020.9264552.

- [83] H. Ramezani and R. Benekohal, "Optimized speed harmonization with connected vehicles for work zones," in *Proc. 2015 IEEE 18th Int. Conf. Intell. Transp. Syst.*, pp. 1081–1086, doi: 10.1109/ITSC.2015.179.
- [84] J. Ma et al., "Freeway speed harmonization," *IEEE Trans. Intell. Veh.*, vol. 1, no. 1, pp. 78–89, Mar. 2016, doi: 10.1109/TIV.2016.2551540.
- [85] A. A. Malikopoulos, S. Hong, B. B. Park, J. Lee, and S. Ryu, "Optimal control for speed harmonization of automated vehicles," *IEEE Trans. Intell. Transp. Syst.*, vol. 20, no. 7, pp. 2405–2417, Jul. 2019, doi: 10.1109/TITS.2018.2865561.
- [86] G. Piacentini, A. Ferrara, I. Papamichail, and M. Papageorgiou, "Highway traffic control with moving bottlenecks of connected and automated vehicles for travel time reduction," in *Proc. 2019 IEEE 58th Conf. Decis. Control (CDC)*, pp. 3140–3145, doi: 10.1109/CDC40024.2019.9029994.
- [87] H. M. Abdelghaffar, M. Elouni, Y. Bichiou, and H. A. Rakha, "Development of a connected vehicle dynamic freeway variable speed controller," *IEEE Access*, vol. 8, pp. 99,219–99,226, May 2020, doi: 10.1109/ACCESS.2020.2995552.
- [88] N. Goulet and B. Ayalew, "Distributed maneuver planning with connected and automated vehicles for boosting traffic efficiency," *IEEE Trans. Intell. Transp. Syst.*, vol. 23, no. 8, pp. 10,887–10,901, Aug 2022, doi: 10.1109/TITS.2021.3096878.
- [89] C. H. Nguyen, N. H. Hoang, S. Lee, and H. L. Vu, "A system optimal speed advisory framework for a network of connected and autonomous vehicles," *IEEE Trans. Intell. Transp. Syst.*, vol. 23, no. 6, pp. 5727–5739, Jun. 2022, doi: 10.1109/TITS.2021.3056696.
- [90] A. R. Kreidieh, C. Wu, and A. M. Bayen, "Dissipating stop-and-go waves in closed and open networks via deep reinforcement learning," in *Proc. 2018 21st Int. Conf. Intell. Transp. Syst. (ITSC)*, pp. 1475–1480, doi: 10.1109/ITSC.2018.8569485.
- [91] E. Vinitzky, K. Parvate, A. Kreidieh, C. Wu, and A. Bayen, "Lagrangian control through deep-RL: Applications to bottleneck decongestion," in *Proc. 2018 21st Int. Conf. Intell. Transp. Syst. (ITSC)*, pp. 759–765, doi: 10.1109/ITSC.2018.8569615.
- [92] H. Xia, K. Boriboonsomsin, and M. Barth, "Dynamic eco-driving for signalized arterial corridors and its indirect network-wide energy/emissions benefits," *J. Intell. Transp. Syst.*, vol. 17, no. 1, pp. 31–41, 2013, doi: 10.1080/15472450.2012.712494.
- [93] C. Roncoli, M. Papageorgiou, and I. Papamichail, "Traffic flow optimisation in presence of vehicle automation and communication systems—Part II: Optimal control for multi-lane motorways," *Transp. Res. C, Emerg. Technol.*, vol. 57, pp. 260–275, Aug. 2015, doi: 10.1016/j.trc.2015.05.011.
- [94] C. Roncoli, I. Papamichail, and M. Papageorgiou, "Hierarchical model predictive control for multi-lane motorways in presence of vehicle automation and communication systems," *Transp. Res. C, Emerg. Technol.*, vol. 62, pp. 117–132, Jan. 2016, doi: 10.1016/j.trc.2015.11.008.
- [95] L. Zhao and A. A. Malikopoulos, "Decentralized optimal control of connected and automated vehicles in a corridor," in *Proc. 21st Int. Conf. Intell. Transp. Syst. (ITSC)*, Nov. 2018, pp. 1252–1257, doi: 10.1109/ITSC.2018.8569229.
- [96] A. M. I. Mahbub, A. A. Malikopoulos, and L. Zhao, "Impact of connected and automated vehicles in a corridor," in *Proc. 2020 Amer. Control Conf.*, pp. 1185–1190, doi: 10.23919/ACC45564.2020.9147678.
- [97] A. I. Mahbub, A. A. Malikopoulos, and L. Zhao, "Decentralized optimal coordination of connected and automated vehicles for multiple traffic scenarios," *Automatica*, vol. 117, p. 108,958, Jul. 2020, doi: 10.1016/j.automatica.2020.108958.
- [98] A. M. I. Mahbub and A. A. Malikopoulos, "Concurrent optimization of vehicle dynamics and powertrain operation using connectivity and automation," SAE International, Warrendale, PA, USA, SAE Tech. Paper 2020-01-0580, 2020.
- [99] J. Rios-Torres and A. A. Malikopoulos, "A survey on coordination of connected and automated vehicles at intersections and merging at highway on-ramps," *IEEE Trans. Intell. Transp. Syst.*, vol. 18, no. 5, pp. 1066–1077, May 2017, doi: 10.1109/TITS.2016.2600504.
- [100] J. Guanetti, Y. Kim, and F. Borrelli, "Control of connected and automated vehicles: State of the art and future challenges," *Annu. Rev. Control*, vol. 45, pp. 18–40, Apr. 2018, doi: 10.1016/j.arcontrol.2018.04.011.
- [101] P. Grim, R. Rosenberger, A. Rosenfeld, B. Anderson, and R. E. Eason, "How simulations fail," *Synthese*, vol. 190, no. 12, pp. 2367–2390, 2013, doi: 10.1007/s11229-011-9976-7.
- [102] M. Pahlavan, M. Papatriantafylou, and E. M. Schiller, "Gulliver: A testbed for developing, demonstrating and prototyping vehicular systems," in *Proc. 9th ACM Int. Symp. Mobility Manage. Wireless Access*, 2011, pp. 1–8, doi: 10.1145/2069131.2069133.
- [103] J. Axelsson, A. Kobetski, Z. Ni, S. Zhang, and E. Johansson, "Moped: A mobile open platform for experimental design of cyber-physical systems," in *Proc. 2014 40th EUROMICRO Conf. Softw. Eng. Adv. Appl.*, pp. 423–430, doi: 10.1109/SEAA.2014.38.
- [104] L. Paull et al., "Duckietown: An open, inexpensive and flexible platform for autonomy education and research," in *Proc. IEEE Int. Conf. Robot. Autom.*, 2017, pp. 1497–1504, doi: 10.1109/ICRA.2017.7989179.
- [105] S. Kannapiran and S. Berman, "Go-chart: A miniature remotely accessible self-driving car robot," in *Proc. 2020 IEEE/RSJ Int. Conf. Intell. Robots Syst. (IROS)*, pp. 2265–2272, doi: 10.1109/IROS45743.2020.9341770.
- [106] N. Hyaldmar, Y. He, and A. Porok, "A fleet of miniature cars for experiments in cooperative driving," in *Proc. IEEE Int. Conf. Robot. Autom.*, 2019, pp. 3238–3244, doi: 10.1109/ICRA.2019.8794445.
- [107] S. Wilson et al., "The robotarium: Globally impactful opportunities, and lessons learned in remote-access, distributed control of multirobot systems," *IEEE Control Syst. Mag.*, vol. 40, no. 1, pp. 26–44, Feb. 2020, doi: 10.1109/MCS.2019.2949973.
- [108] M. Kloock et al., "Cyber-physical mobility lab an open-source platform for networked and autonomous vehicles," 2020, *arXiv:2004.10063*.
- [109] A. Jiménez-González, J. R. Martínez-de Dios, and A. Ollero, "Testbeds for ubiquitous robotics: A survey," *Robot. Auton. Syst.*, vol. 61, no. 12, pp. 1487–1501, 2013, doi: 10.1016/j.robot.2013.07.006.
- [110] R. M. Zayas, L. E. Beaver, B. Chalaki, H. Bang, and A. A. Malikopoulos, "A digital smart city for emerging mobility systems," 2021, *arXiv:2109.02811*.
- [111] A. M. I. Mahbub, V. Karri, D. Parikh, S. Jade, and A. A. Malikopoulos, "A decentralized time- and energy-optimal control framework for connected automated vehicles: From simulation to field test," SAE International, Warrendale, PA, USA, SAE Tech. Paper 2020-01-0579, 2020.
- [112] *Human-Driven Robotic Car*. (Feb. 27, 2019). [Online Video]. Available: <https://www.youtube.com/watch?v=f5ZRQLLQirE>
- [113] L. Zhao, A. A. Malikopoulos, and J. Rios-Torres, "On the traffic impacts of optimally controlled connected and automated vehicles," in *Proc. 2019 IEEE Conf. Control Technol. Appl.*, pp. 882–887, doi: 10.1109/CCTA.2019.8920630.
- [114] M. Ratnagiri, C. O'Dwyer, L. E. Beaver, B. Chalaki, H. Bang, and A. A. Malikopoulos, "A scalable last-mile delivery service: From simulation to scaled experiment," 2021, *arXiv:2109.05995*.
- [115] B. Remer and A. A. Malikopoulos, "The multi-objective dynamic traveling salesman problem: Last mile delivery with unmanned aerial vehicles assistance," in *Proc. 2019 Amer. Control Conf. (ACC)*, pp. 5304–5309, doi: 10.23919/ACC.2019.8815099.
- [116] L. E. Beaver, B. Chalaki, A. M. Mahbub, L. Zhao, R. Zayas, and A. A. Malikopoulos, "Demonstration of a time-efficient mobility system using a scaled smart city," *Veh. Syst. Dyn.*, vol. 58, no. 5, pp. 787–804, 2020, doi: 10.1080/00423114.2020.1730412.
- [117] B. Chalaki and A. A. Malikopoulos, "Robust learning-based trajectory planning for emerging mobility systems," in *Proc. 2022 Amer. Control Conf. (ACC)*, pp. 2154–2159, doi: 10.23919/ACC53348.2022.9867265.
- [118] A. M. I. Mahbub and A. A. Malikopoulos, "Conditions to provable system-wide optimal coordination of connected and automated vehicles," *Automatica*, vol. 131, p. 109,751, Sep. 2021, doi: 10.1016/j.automatica.2021.109751.
- [119] G. R. de Campos, P. Falcone, and J. Sjöberg, "Autonomous cooperative driving: A velocity-based negotiation approach for intersection crossing," in *Proc. 16th Int. IEEE Conf. Intell. Transp. Syst. (ITSC)*, 2013, pp. 1456–1461, doi: 10.1109/ITSC.2013.6728435.
- [120] B. Chalaki and A. A. Malikopoulos, "A priority-aware replanning and rescheduling framework for coordination of connected and automated vehicles," *IEEE Control Syst. Lett.*, vol. 6, pp. 1772–1777, 2022, doi: 10.1109/LCSYS.2021.3133416.
- [121] M. Treiber, A. Hennecke, and D. Helbing, "Congested traffic states in empirical observations and microscopic simulations," *Phys. Rev. E*, vol. 62, no. 2, p. 1805, 2000, doi: 10.1103/PhysRevE.62.1805.
- [122] A. M. I. Mahbub, B. Chalaki, and A. A. Malikopoulos, "A constrained optimal control framework for vehicle platoons with delayed communication," 2022, *arXiv:2111.08080*.
- [123] L. E. Beaver and A. A. Malikopoulos, "Constraint-driven optimal control of multi-agent systems: A highway platooning case study," *IEEE Control Syst. Lett.*, vol. 6, pp. 1754–1759, 2022, doi: 10.1109/LCSYS.2021.3133801.